Energy-Efficient Speed Planning Considering Delay and Dynamic Waterway Conditions for Inland Vessels

Ir. S Slagter[a*], Dr. Ir. Y Pang[a], Prof. Dr. R R Negenborn[a]

[a]*Delft University of Technology, The Netherlands*

[*]Corresponding author. Email: s.slagter@tudelft.nl

Synopsis

The inland waterway transport sector is facing increasingly stringent legislation to reduce emissions and improve energy efficiency. Speed planning methods are an attractive option as they provide energy-efficient, timely and emission-reducing voyage planning for ships. However, current methods do not consider dynamic conditions of waterways and traffic. Due to these dynamic navigational conditions the static speed planning methods do not guarantee optimality, nor do they satisfy the constraints of the optimization problem throughout the journey. In this paper we propose an optimization structure that is based on the Model Predictive Control algorithm, which uses the most current information on water depth, water speed and expected delays to re-optimize the speed planning throughout the journey. Through a use case we show a 4.31% energy reduction compared to other speed planning strategies. Additionally, we show that the constraints regarding desired arrival times and safety are satisfied throughout the journey. Therefore, the method proves useful from a logistical, energy, emissions, and safety perspective. Modelling of uncertainties, lock interactions and predictions of waterway conditions will make our method an even more attractive option for speed planning.

Keywords: Voyage optimization; Non-linear control systems; Model predictive control; Inland shipping

1 Introduction

1.1 Background

Each industry and transport sector must change in order to meet the goals set out by the European Commission in the European Green Deal. This legislation aims to reduce the net greenhouse gas emissions by 55% by 2030, and to be climate-neutral by 2050 (EC, 2020).The Commission has also set an 'energy efficiency target of reducing final energy consumption by at least 11.7% compared to projections of the expected energy use for 2030' (EC, 2022). Improving energy efficiency is a critical strategy for mitigating environmental impact, conserving natural resources, and promoting a more sustainable business practise. Using energy more efficiently reduces the amount of energy required, thereby lowering emissions and mitigating environmental damage.

For the inland waterway transport (IWT) sector the NAIADES III action plan is established which states various goals for the sector such as lowering emissions and achieving smarter waterways (EC, 2021). The IWT sector is dedicating much research into clarifying transition pathways (CCNR, 2022; Kirichek et al., 2024), developing novel technologies to facilitate the transition, and developing methods to improve the energy efficiency of ships in operation. Our interest lies in the energy efficient methods for ship operations as these solution will be immediately applicable, and remain valuable during and after the energy transition; even with zero emission technology, we still want to reduce the required energy for operations.

A method of particular interest is voyage optimization, which is a method that aims to provide safe, energy-efficient, timely and emission-reducing voyage planning for ships. Additionally, they directly contribute to achieving smarter inland waterways (EC, 2021), and are relatively cost-effective and simple to implement leading to little or no downtime upon implementation. Inland shipping frequently relies on a single route from start to finish, resulting in a focus on speed planning rather than the combined optimization of speed and route due to limited route options. For that reason, voyage optimization for inland shipping is often reduced to speed optimization.

1.2 Related works and research gap

Speed planning for inland shipping involves finding the optimal speed setpoints along the journey as a function of ship design parameters, traffic and fairway conditions, cargo, and powertrain characteristics. Methods as

Authors' Biographies

Ir. Simeon Slagter is a PhD candidate at the section Transport Engineering & Logistics of the department Maritime & Transport Technology, Delft University of Technology. Ir. Slagter's research interests include intelligent control for ship operations to improve the energy efficiency of inland vessels and the maritime energy transition.

Dr. Ir. Yusong Pang is assistant professor at the section Transport Engineering & Logistics of the department Maritime & Transport Technology, Delft University of Technology. Dr. Pang's research interests include intelligent control and monitoring of operations for applications of transport and production processes.

Prof. Dr. Rudy R Negenborn is full professor in Multi-Machine Operations & Logistics at Delft University of Technology. He is head of the Section Transport Engineering & Logistics, and leads the Researchlab Autonomous Shipping (RAS). Prof. Negenborn's research interests include multi-agent systems, distributed control, model predictive control for applications in (waterborne) networked transport systems.

 https://doi.org/10.24868/11161

presented in (Yan et al., 2018; WANG et al., 2019) discretize the journey in different segments or legs. Then, for each of these segments the optimal speed setting for the engine or ship is found for which the energy is minimized over the journey, resulting in a 2-5% energy reduction. Similarly, (Fan et al., 2021) determines the optimal speed setpoints between ports visited on a journey.

Speed is sometimes also co-optimized with energy directly, such as in the works of (Sun et al., 2023; Zhang et al., 2023); they consider the effect of engine setpoints on performance rather than just fairway and journey conditions. Some works take into account environmental conditions such as wind, wave, current velocity, and water depth and their effect on the resistance of the ship (Han et al., 2021; Zhang et al., 2022); others take into account the navigational conditions of the ship, ship specifications, manoeuvring and time windows constraints (Liu, 2023). (Wang et al., 2023) developed a speed planning method that considers maximum allowable SO_x emissions in emission control areas. (Gao et al., 2022) suggests a different voyage optimization, namely trim optimization leading to an energy efficiency of 1.46%.

The field of energy-efficient speed planning for inland vessels is not yet well explored compared to the maritime field. What is currently still missing in literature are methods that consider time-varying environmental and fairway conditions and their uncertainty. During an inland waterway journey the states of water depth and current will change. Additionally, the ship will run into delays at locks, or traffic delays in crowded fairways. Due to these dynamic navigational conditions the speed planning computed at the start of the journey will not remain optimal for long, nor does it guarantee to satisfy the constraints of the optimization problem. For instance, with unexpected delays or higher water speed than anticipated the journey can take substantially longer than anticipated leading to logistical problems such as late arrival times. For this reason, it is important to continually update the speed planning to take into account the most current information on water depth, current velocity, expected delays and experienced delays. Additionally, using accurate and up-to-date information on water depth is particularly important from a safety point of view; low water depths can cause grounding, higher water depths can cause safety concerns at bridges.

1.3 Aim and contribution

Dynamic waterway conditions and delays have not yet been considered in speed planning for inland vessels. It is our aim to provide a framework in which these conditions are taken into account. For that reason, in this work we propose an optimization structure that is based on the Model Predictive Control (MPC) algorithm, which continually uses the most up-to-date information throughout the journey on fairway characteristics and delays to re-optimize the speed planning, leading to improved energy efficiency, reliable arrival times, and satisfied constraints.

1.4 Structure of the paper

In Section 2 we provide the static speed planning model consisting of the resistance modelling of an inland vessel in shallow waters, models for estimating the energy consumption and the objective function and constraints of the speed planning model. Secondly, in Section 3 we introduce the MPC framework of the dynamic speed planning model and the updating procedure for different dynamic constraints and parameters. In Section 4 we define a use case and explain the dynamic parameters, journey parameters, and ship characteristics. In Section 5 the results of the case study are shown and discussed. The results are compared to other speed planning strategies to show the energy efficiency of the method. Additionally, a sensitivity analysis is included to show the effects of the dynamic parameters on the energy consumption. Finally, in Section 6 are the conclusions and suggestions for further research.

2 Speed planning model

In this paper we introduce a stretch-based speed planning model tailored for inland waterway navigation. We segment the journey from origin to destination into discrete stretches, each characterized by specific fairway features like water depth and current speed. The goal of this model is to determine the most energy-efficient speed for each stretch, minimizing the ship's overall energy consumption, while satisfying journey constraints. The speed planning model consists of three main parts: 1. Resistance models of a ship in shallow water; 2. Models for estimating resultant energy consumption; 3. An objective function and associated constraints that define the optimization problem.

2.1 Resistance modelling of an inland vessel in shallow waters

To maintain a particular sailing speed the ship's engine must provide a certain power to drive the propeller to provide a certain thrust that is able to overcome the resistances acting on the ship. The resistances on the ship can be modelled using the Holtrop and Mennen estimations (Holtrop and Mennen, 1982):

$$R_T^n = R_F^n(1+k_1) + R_W^n + R_{APP}^n + R_{TR}^n + R_A^n + R_B^n \quad \forall \quad n \in \mathrm{N} \tag{1}$$

 https://doi.org/10.24868/11161

where R_T is the total resistance acting on the ship; R_F is the frictional resistance; R_{APP} is appendage resistance; R_W is the wave-making and breaking resistance, calculated based on the Froude number (Holtrop, 1984); R_B is the additional resistance due to the bulbous bow. For inland vessels $R_B = 0$ since most inland vessels do not have a bulbous bow; R_{TR} is the additional resistance due to an immersed transom; R_A is model-ship correlation resistance; and k1 is the viscous resistance factor for different ship types. All of these resistances will be calculated for each stretch n. Therefore, R_T^n is the total resistance acting on the ship on stretch n of the journey. The set of n stretches is N.

$$N = \{1, 2, 3, ..., n\} \tag{2}$$

The frictional resistance of the ship can be calculated using:

$$R_f^n = \frac{1}{2}\rho (V_s^n)^2 C_f^n S \quad \forall \quad n \in \mathrm{N} \tag{3}$$

in which ρ is the density of water [kg/m^3]; V_s is the speed of the vessel over water [m/s]; C_f is the friction coefficient; S is the wetted surface area of the hull [m^2]. To model the friction coefficient for shallow waters as accurately as possible we use the method proposed by (Zeng, 2019). The method adjusts the friction coefficient to take into account both the additive friction resistance below the ship in shallow waters as well as the friction at the submerged flanks of the ship. The method estimates the velocity underneath the ships bottom with:

$$V_s^n + \Delta V_n = 0.4277 \cdot V_s^n \cdot \exp\left(\frac{h_n}{D_s}\right)^{-0.07634} \quad \forall \quad n \in \mathrm{N}, \tag{4}$$

in which h_n is the water depth on stretch n, and D_s is the draft of the ship. The reported uncertainty of this formula is 2.5% (Zeng, 2019), and it is only suitable for $\frac{h_n}{D_s} \leq 4$. For $\frac{h_n}{D_s} \geq 4$, $V_s^n + \Delta V_n$ is assumed to be equal to V_s^n (van Koningsveld et al., 2021). The remaining resistance components are calculated according to the Holtrop and Mennen models (Holtrop and Mennen, 1982).

2.2 Models for Energy estimation

The second part of the speed planning method relates the resistances on the ship to required power, energy consumption, and travel duration. The effective power to overcome the resistances on the ship can be modelled with equation 5 (Wang et al., 2021).

$$P_E^n = k \cdot R_T^n \cdot V_s^n \quad \forall \quad n \in \mathrm{N} \tag{5}$$

In which P_E^n is the effective power to overcome the resistance and k is the number of propellers. For inland shipping k is usually one. The delivered power to propellers P_D^n is larger than the required effective power because of efficiency of the propeller in open water η_O, relative rotation efficiency η_R, and the hull efficiency η_H.

$$P_D^n = P_E^n / (\eta_O \cdot \eta_R \cdot \eta_H) \quad \forall \quad n \in \mathrm{N} \tag{6}$$

These three efficiencies together make up the hydrodynamic efficiency of the ship η_D^n (Simić and Radojcic, 2013).

$$\eta_D = \eta_O \cdot \eta_R \cdot \eta_H \quad \forall \quad n \in \mathrm{N} \tag{7}$$

The propeller behaves differently for different water depths resulting in different efficiency ratings. In this work we assume a hydrodynamic efficiency of between 0.35 and 0.5 dependant on the water depth (Jiang et al., 2022; Simić and Radojcic, 2013). The main engine power output P_B is related to the delivered power at the propeller through the shaft efficiency η_S and the gearbox efficiency η_G.

$$P_B^n = P_D^n / (\eta_S \cdot \eta_G) \quad \forall \quad n \in \mathrm{N} \tag{8}$$

The expected energy consumption on stretch n is E_n^* and can be estimated using equation 9.

$$E_n^* = P_B^n \cdot t_n^* \quad \forall \quad n \in \mathrm{N} \tag{9}$$

In which t_n^* is the expected sailing duration [h] on stretch n, and can be estimated by relating distance travelled, d [m], and speed over ground, V_{og}:

$$t_n^* = \frac{d_n \cdot \phi_n^*}{3600 V_{og}^n} \quad \forall \quad n \in \mathrm{N} \tag{10}$$

in which ϕ_n^* is a parameter denoting expected delay on stretch n. The speed over ground can be inferred by the ship speed and current velocity, V_c [m/s]. In this formula the current direction is taken as positive when flowing in the same sailing direction as the ship.

$$V_{og}^n = V_s^n + V_c^n \quad \forall \quad n \in \mathrm{N} \tag{11}$$

 https://doi.org/10.24868/11161

The total expected energy consumption during the trip, E^*_{trip} [kWh], is the sum of the expected energy consumption on the stretches:

$$E^*_{trip} = \sum_{n=1}^{N} E^*_n. \tag{12}$$

Similarly, the total expected travel duration, t^*_{trip} [h], is the sum of the expected travel duration on each stretch n:

$$t^*_{trip} = \sum_{n=1}^{N} t^*_n \tag{13}$$

Finally, we define an expected arrival time t_{n^*} at each stretch n using the equation below.

$$t_{n^*} = \sum_{n=1}^{n^*-1} t^*_n \quad \forall \quad n^* \in \mathrm{N}, n^* \neq 1 \tag{14}$$

For the arrival time at stretch 1 ($n^* = 1$) the arrival time is zero $t_{n^*} = 0$. Using this formulation we can impose window arrival time constraints.

2.3 Objective function and constraints

Constraints are applied on the following state and decision variables which may be selected by end-user preference to ensure a maximum travel time (equation 15), arrival windows (equation 16), and energy consumption (equation 17).

$$t_{trip,min} \leq t^*_{trip} \leq t_{trip,max} \tag{15}$$

$$t_{n^*,min} \leq t_{n^*} \leq t_{n^*,max} \tag{16}$$

$$E^*_{trip} \leq E_{trip,max} \tag{17}$$

Constraints on the minimum and maximum speed over ground is imposed also. These bounds take into account the physical restriction on speed given the installed engines and water depth, and speed limits on fairways.

$$V^n_{s,min} \leq V^n_s \leq V^n_{s,max} \quad \forall \quad n \in \mathrm{N} \tag{18}$$

Indirectly, a speed limit is also imposed through a safety constraint that takes into account the squat effect of the ship, aiming to maintain a minimum clearance γ between the ship and the bottom of the fairway. We calculate squat s_n taking into account the width and depth of the river (Serban et al., 2015).

$$s_n = K \cdot C_B \cdot (V^n_s)^2/100 \quad \forall \quad n \in \mathrm{N} \tag{19}$$

In which K is function of the fairway characteristics such as depth, width and shape (Serban et al., 2015); C_B is the block coefficient. We assume a block coefficient of 0.85 for inland vessels. We pose that the sum of ship draft D_s, squat s_n and minimum clearance γ should be smaller than the depth of the river h_n; which leads to the safety constraint, equation 20.

$$D_s + s_n + \gamma \leq h_n \quad \forall \quad n \in \mathrm{N} \tag{20}$$

Finally, the objective function aims to minimize the energy consumption over the whole journey and has the form:

$$min_{\overrightarrow{u}}\, J = E^*_{trip}, \tag{21}$$

where $\overrightarrow{u}$ represent the set of decision variables of the problem formulation.

$$\overrightarrow{u} = \begin{pmatrix} V^1_s \\ \dots \\ V^n_s \end{pmatrix} \tag{22}$$

3 Optimization method involving dynamic fairway and delay conditions

In this work we propose an optimization structure that is based on the Model Predictive Control (MPC) algorithm, which continually uses the most up-to-date information on fairway characteristics and delays of the journey, to re-optimize the speed planning. The algorithm used for this optimization scheme is shown in Table 1. In the first step, the system is initialised; the ship parameters, journey parameters and constraints are loaded. Secondly, on the first iteration of the for-loop the speed planning is computed for the complete journey (origin to destination). The

 https://doi.org/10.24868/11161

first step of the optimal solution set $\overrightarrow{u}^*$ is carried out; the first stretch of the journey is travelled using the suggested speed from the speed planning. After each stretch of the journey the speed plan is re-optimized for the remainder of the journey, taking into account the actual delays ϕ_n, updated expected delays ϕ_n^*, and most current information on water depth h_n and current velocity V_c^n. The optimization problem shrinks after each re-optimization, since we do not to consider stretches that have already been travelled in the new speed planning. To account for the encountered delays the actual travel time t_n is calculated using:

$$t_n = \frac{d_n \cdot \phi_n}{3600 V_{og}^n} \quad \forall \quad n \in \mathrm{N} \tag{23}$$

The actual energy consumption E_n is:

$$E_n = P_B^n \cdot t_n \quad \forall \quad n \in \mathrm{N} \tag{24}$$

Since the optimization problem shrinks after each stretch travelled, the constraint parameters must be updated also; this ensures that the initial constraints set at the start of the journey remain satisfied throughout the dynamic changes of the journey. The updating function of these parameters are as described below in equations 25 to 29. These functions are executed in each iteration of step 6 of the algorithm described in Table 1.

$$t_{trip,max} = t_{trip,max} - t_n \tag{25}$$

$$t_{trip,min} = t_{trip,min} - t_n \tag{26}$$

$$t_{n^*,min} = t_{n^*,min} - t_n \tag{27}$$

$$t_{n^*,max} = t_{n^*,max} - t_n \tag{28}$$

$$E_{trip,max} = E_{trip,max} - E_n \tag{29}$$

The optimization problem is a constraint non-linear optimization problem. We solve the optimization problem using a sequential quadratic programming approach. A common difficulty with non-linear optimization problems is finding the global optimum since the complex solution space might lead to local optima. To overcome this issue we use a multi-start procedure; we do the optimization procedure multiple times with different initial solutions. For the use-case described in this paper this guarantees the optimal solution is found.

Table 1: The dynamic optimization algorithm based on the MPC strategy

The dynamic optimization algorithm based on the MPC strategy.
1. At timestep n=1 initialise the system; define ship parameters, set origin and destination of journey, load fairway characteristics, set the desired constraints, define the objective function, and define the problem size: z = size(N).
2. **For** n = 1:z
3. Load current information on water depth h_n, current velocity V_c^n and expected delays ϕ_n^*. Initialise the optimization problem for stretches n to z.
4. Solve the constraint non-linear optimization problem using sequential quadratic programming, and a multi-start procedure to guarantee successful convergence to the global optimum; equations 1 to 21.
5. The first step of the optimal solution set $\overrightarrow{u}^*$ is carried out. The experienced (real) delay ϕ_n and actual travel time t_n are recorded.
6. The constraints on maximum arrival times, arrival windows and maximum energy consumption are updated according to equations 25 to 29.
7. n = n + 1, return to step 2
End for-loop

4 Case study

To exemplify the method presented in the previous section and to validate the approach we study a use case; a CEMT class Va inland freight vessel sailing the Rhine upstream from Rotterdam (Netherlands) to Basel (Switzerland) for a total distance of 829 km. Graphically the journey is shown in Figure 1. The speed planning method determines the appropriate vessel sailing speed on each of the stretches of the journey, for which all imposed constraints are satisfied and energy consumption is minimized. By determining the vessel speed on a 'stretch-level', we can ensure the energy efficiency over the journey is achieved while considering the varying conditions of water depth and currents locally. The navigation circumstances of passing locks between Karlsruhe and Basel, and vessel crossings are not considered directly in this framework. However, the traffic delay parameter ϕ^* is used to model

 https://doi.org/10.24868/11161

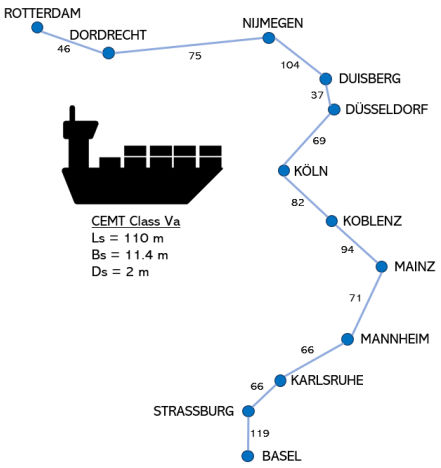

Figure 1: The journey from Rotterdam to Basel and the discretization of the journey in 11 edges; for each edge the length is displayed in km.

the expected delay on each stretch of the journey. All the relevant journey, ship, engine, and constraint parameters of the use-case are summarized in Table 2.

The water levels in the use case are initially low, with a smallest water depth of 2.4 m between Düsseldorf and Köln. These numbers are representative based on reports of CCNR and the Prominent project (TNO et al., 2016; Orlovius, 1994). Over time as the ship completes the journey the water depth changes. In Table 2 the water depth at the the final moment (t_f) of the journey is given as $h_n(t_f)$. In this use case the journey lasts 90 hours ($t_{trip,max} = t_f$). Throughout this journey the water depth slowly transitions between initial and final state. Therefore, when the ship travels stretch n the actual water depth encountered is $h_n(t_{n^*})$ which is between $h_n(0)$ and $h_n(t_f)$. The average expected water depth at $t = 0$ and the actual encountered average water depth of the use case are shown in Table 3. Similarly, the current velocity has an initial and final state and throughout the journey the states slowly change. Finally, the expected and real delay do not match exactly. The average expected and actual values for water depth, current and delay can be found in Table 3.

 https://doi.org/10.24868/11161

Table 2: The summary of all the use case parameters.

Parameter	**Variable**	**Value**
	Journey parameters	
Origin		Rotterdam, Netherlands
Destination		Basel, Switzerland
Total travel distance [km]	d_{trip}	829
Set of stretches [-]	N	$\{1, 2, 3, 4, 5, 6, 7, 8, 9, 10, 11\}$
Stretch lengths [km]	d_n	[46, 75, 104, 37, 69, 82, 94, 71, 66, 66, 119]
Stretch water depth [m] at $t = 0$	$h_n(0)$	[9, 6, 5, 3, 2.4, 2.8, 3, 2.7, 3, 3, 3]
Stretch water depth [m] at $t = t_f$	$h_n(t_f)$	[9.21, 6.23, 5.26, 3.28, 2.71, 3.14, 3.36, 3.08, 3.42, 3.47, 3.50]
Stretch current velocity [m/s] at $t = 0$	$V_c^n(0)$	[-0.83, -0.83, -1.11, -1.11, -1.38, -1.66, -1.66, -1.66, -1.66, -1.94, -1.94]
Stretch current velocity [m/s] at $t = t_f$	$V_c^n(t_f)$	[-0.66, -0.66, -0.94, -0.94, -1.21, -1.49, -1.49, -1.49, -1.49, -1.77, -1.77]
Expected delay [-]	$\phi_n^* \; \forall n \in N$	1.05
Actual delay [-]	ϕ_n	[1.03, 1.05, 1.02, 1.03, 1.03, 1.03 , 1.04, 1.02, 1.04, 1.04, 1.02]
	Ship parameters	
Ship type		CEMT Class Va inland freight vessel
Length at waterline [m]	L_s	110
Beam [m]	B_s	11.4
Draft [m]	D_s	2.0
Block coefficient [-]	C_B	0.85
Transom area [m^2]	A_T	4.56
Wetted area appendages [m^2]	S_{app}	72.45
Appendage resistance factor [-]	1+k2	2.5
Hydrodynamic efficiency [-]	η_d	0.35 - 0.53
	General parameters	
Gravitational constant [m/s^2]	g	9.81
Water density [kg/m^3]	ρ	1000
Kinematic viscosity of water [m^2/s]	υ	$1.1296 \cdot 10^{-}6$
Wave resistance parameter [-]	d	-0.9
	Engine and powertrain parameters	
Gearing efficiency [-]	η_G	0.96
Shaft efficiency [-]	η_S	0.98
	Constraint parameters	
Maximum speed [km/h]	$V_{s,max}^n \; \forall n \in N$	18
Minimum speed [km/h]	$V_{s,min}^n \; \forall n \in N$	6 - $V_c^n \cdot 3.6$
Maximum arrival time [h]	$t_{trip,max}$	90
Minimum arrival time [h]	$t_{trip,min}$	0
Minimum window arrival time [h]	$t_{n^*,min} \; \forall n \in N$	$t_{trip,min}$
Maximum window arrival time [h]	$t_{n^*,max} \; \forall n \in N$	$t_{trip,max}$
Minimum clearance [m]	γ	0.3

We impose a static vessel speed limit of 18 km/h for the ship, and a minimum vessel speed of 6 km/h minus the current velocity. Therefore, for whichever current, the minimum speed over ground will be 6 km/h. The static speed constraint of 18 km/h is to take into account the maximum capabilities of the ship. The safety constraint (function 20) which imposes a minimum clearance of $\gamma = 0.3m$ (De Ruiter et al., 2023) between the ship and the river bottom considering the squat effect, indirectly imposes a dynamic speed limit also. For that reason, in shallow waters the ship will not always be able go at maximum speed because it will impose a squat effect that is considered unsafe. We impose a maximum trip duration of 90 hours as this will lead to common speed ranges of ships on the Rhine (De Ruiter et al., 2023); this makes our use case more comparable to real-world practise.

Table 3: Average values of dynamic parameters at the initial state and encountered states

Parameter	Mean value at t = 0	Mean value of actual encountered dynamic conditions	Difference [%]
Water depth h_n	3.9 m	4.07 m	4.36
Current velocity V_c^n	-5.18 km/h	-4.87 km/h	-5.98
Delay ϕ_n	1.05	1.03	-1.90

 https://doi.org/10.24868/11161

5 Results and discussion

The optimal sailing speed for each stretch of the journey at each time step along the route is shown in Table 4. At each timestep for the remaining journey the speed plan is re-optimised to find the best speed settings for which the total energy consumption is minimised. The first row of the table are the sailing speed solutions at timestep 1; this is the speed plan that is suggested at the start of the journey. If the speed planning is static, this will be the speed plan that is executed throughout the journey. The solutions of our dynamic speed planning framework are on the diagonal of the table.

Table 4: The optimal sailing speeds at each time step along the route

Time	Journey segments										
steps n	1	2	3	4	5	6	7	8	9	10	11
1	15.36	14.94	15.22	14.70	11.46	15.59	15.78	15.53	15.78	16.27	16.27
2		14.82	15.17	14.64	11.46	15.51	15.59	15.47	15.59	16.24	16.24
3			15.07	14.55	11.46	15.42	15.48	15.41	15.50	16.19	16.19
4				14.38	11.46	15.30	15.35	15.29	15.36	16.09	16.08
5					13.96	14.78	14.89	14.76	14.91	15.42	15.41
6						14.69	14.76	14.68	14.78	15.36	15.35
7							14.65	14.59	14.66	15.29	15.28
8								14.49	14.56	15.21	15.20
9									14.44	15.06	15.07
10										14.95	14.97
11											14.85

It can be noted that the speed suggestions are descending in value over time. This follows naturally from a current velocity that is decreasing over time and the overestimation of the delay, see Table 3. It should also be noted that the speed setting on journey segment 5 is lower than most setpoints. This is due to the low water depth on this stretch of the journey leading to forcing constraints on maximum vessel speed on this segment to ensure grounding does not occur. However, since the water depth is increasing over time, by the time the ship arrives at segment 5 the speed can be raised while a minimum clearance γ of 0.30 m is maintained.

We cannot directly compare the energy consumption of static and dynamic (MPC) speed planning, because this would be an 'unfair' comparison as the use-case that we choose strongly influences the amount of energy reductions achievable. In our use case the magnitude of the average current velocity and the expected delays are overestimated, and the water depth is underestimated at the start of the journey. These valuations of the states lead to relatively high speed settings to overcome these unfavorable conditions and to arrive on time. Throughout the journey the true dynamic states emerge to be more favourable: a smaller negative current acting on the ship, a higher water depth, and less traffic delay. Therefore, as we re-optimize at each timestep the speed can be lowered because we are finding that the dynamic states are less adverse than expected; this leads to a lower energy consumption. It is well known that lower velocities lead to lower energy consumption, which is basis of slow steaming techniques (Psaraftis and Kontovas, 2013). Had we chosen a use case where the velocity of the current is under-valuated for instance, we would have seen an increase in suggested speed in the dynamic speed planner, and the resultant energy consumption would be higher.

To illustrate this point we show the sensitivity of the energy consumption to varying conditions of water depth, current and delay. We multiply the initial conditions of these parameters with sensitivity parameter $x \in [0.8, 1.2]$. The results can be found in Figure 2. A linear relationship between current velocity and energy consumption can be noted. Similarly, the delay variation also causes a linear response in the energy consumption. The slope of the delay is smaller because the multiplication factor x with delay parameter $\phi* = 1.05$ yields numbers relatively close to 1, and therefore a smaller change in energy. The increase in water depth has a nonlinear response, leading to lower energy consumption. We did not test a decrease in water depth as this would lead to unsafe navigable waters, and the sensitivity response would not be valid.

To make a 'fairer' comparison we compare 6 different speed planning strategies so that we can make some conclusions about the energy efficiency of the proposed MPC method. These speed planning methods, their speed setpoints, average speed, energy consumption, and travel time are shown in Table 5, and in Table 6 the comparison of the different methods is presented. The first three strategies in the table concern static speed planning. The first strategy is a speed selection by the shipper and does not involve and optimization, these speed settings lead to a total estimated travel time of 90 hours, which is the constraint we set for arrival time. The second strategy is our speed planning method without the MPC function (row 1 of Table 4), again the estimated total travel time is 90 hours. In Table 6 a quick comparison of these two methods show that a 6.56% energy efficiency can be achieved through the static speed planning method. If the shipper had chosen a different combination of speeds the energy efficiency achieved through static speed planning would also change.

 https://doi.org/10.24868/11161

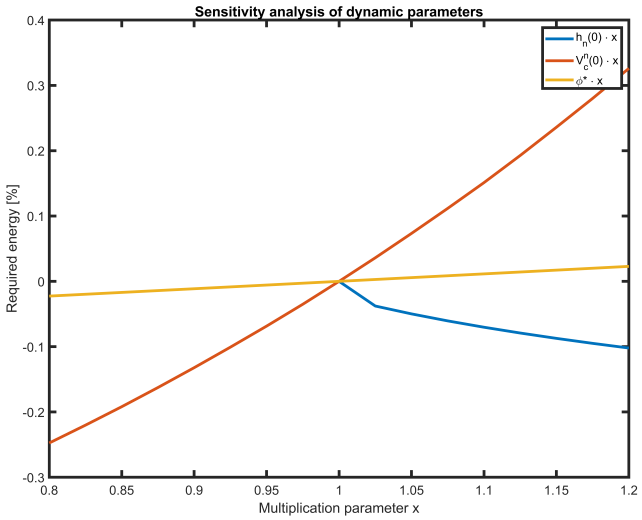

Figure 2: Sensitivity Analysis for the dynamic parameters water depth h_n, current velocity V_c^n, and delay ϕ^*. The base reference in the sensitivity analysis is the speed planning strategy 2 as indicated in Table 5.

Table 5: Overview of different speed planning strategies and their resultant energy efficiency

Speed planning strategy	1	2	3	4	5	6	7	8	9	10	11	Average speed (km/h)	Energy consumption (kWh)	Total travel time (hours)
1. Speed selection by shipper; unassisted by optimization strategies	18.00	18.00	18.00	18.00	11.46	14.40	14.40	14.40	18.00	15.12	15.58	15.81	72525.47	90.00
2. Static speed planning: expected outcome of planning	15.36	14.94	15.22	14.70	11.46	15.59	15.78	15.53	15.78	16.27	16.27	15.27	67767.41	90.00
3. Static speed planning: actual outcome of planning	15.36	14.94	15.22	14.70	11.46	15.59	15.78	15.53	15.78	16.27	16.27	15.27	61618.61	85.10
4. Adaptive speed selection by shipper; unassisted by optimization strategies	18.00	18.00	14.40	14.40	13.00	12.28	15.48	14.40	14.83	15.12	15.58	14.98	59029.54	90.00
5. Dynamic speed planning; optimization with MPC strategy	15.36	14.82	15.07	14.38	13.96	14.69	14.65	14.49	14.44	14.95	14.85	14.71	56485.95	89.56
6. Non-causal optimization: change in water-depth, current and delay is known a priori	14.47	13.95	14.26	13.78	13.90	14.68	14.73	14.63	14.69	15.28	15.27	14.58	55866.42	90.00

Strategy 3 shows the actual outcome of the static speed planning method if the speed planning is followed regardless of the change in water depth, current and delay; it is therefore not really another strategy but rather strategy 2 corrected for dynamic conditions. We can see that the arrival time in reality is 85.10 hours, implying that the average speed could have been lowered during the journey, while still arriving on time. Additionally, due to the reduced velocity of the current, lower than anticipated delay, and higher water depths than anticipated, the energy consumption is 9.07% lower than expected.

Table 6: Comparison of speed planning strategies and their resultant comparative energy savings

Comparison	ΔAverage speed (%)	ΔEnergy use (%)	ΔTime (h)
Strategy 2 compared to 1	-3.42	-6.56	0
Strategy 3 compared to 2	0	-9.07	-4.90
Strategy 5 compared to 3	-3.67	-8.33	+4.46
Strategy 5 compared to 4	-1.80	-4.31	-0.44
Strategy 6 compared to 5	-0.88	-1.10	+0.44

Since it is likely that the shipper will sway from the static speed planning once they notice a delay we include strategy 4. This strategy assumes that the initial speed plan is from strategy 1. However, over time the shipper notices that they are ahead of schedule and that they can lower the speed while still arriving on time. Flexibly, the shipper changes the speed based on the delay experienced in real-time. Strategy 4 will be our point of comparison for the MPC strategy that we propose in the paper, which is strategy 5. Strategy 5, as discussed previously are the

 https://doi.org/10.24868/11161

solution on the diagonal of Table 4. We can note that the arrival time with this strategy is 89.56 hours; it is not exactly equal to 90 hours due to the varying conditions experienced on the final segment of the journey. Compared to strategy 4 we can see that an energy efficiency of 4.31% is achieved. Compared with the static speed planning the MPC method has a 8.33% lower energy consumption.

Finally, strategy 6 shows the non-causal optimization strategy; the exact water depth, current and delay that will be encountered by the ship is known a priori. This strategy shows a 5.36% lower energy consumption as strategy 4. Compared to the MPC strategy is has a 1.10% lower energy consumption. Using prediction models for the current and water depth a speed planning strategy resembling the non-causal optimization may be achieved. However, accurate predictions for a prediction horizon of multiple days may not be feasible. A delay that might be more predictable is at locks using lock planning methods such as described in (Buchem et al., 2022), leading to more precise speed planning. This is also one of the goals of the European (Horizon H2020) NOVIMOVE project (NOVIMOVE, 2020).

It is worth pointing out that the necessity to re-optimize the journey is a reflection of the variation experienced during the journey. Therefore, the energy efficiency percentages achieved with the MPC strategy are a function of the magnitude of the change of the dynamic parameters during the journey. For that reason, lower energy efficiencies will be achieved for journeys with less varying conditions; similarly, with more variations or larger uncertainties higher efficiencies can be achieved. The delays of the use case in this work are quite modest and in reality larger delays may be experienced, especially considering the 10 locks that are in the upper-Rhine. Also, in reality there is often a level of uncertainty about the reported current and water depth. Current velocities of the Rhine can be highly varying in bends for instance, compared to straight parts of the river. For that reason, it is always advisable to update the voyage plan continuously, and to constantly receive the most current estimations on waiting times at locks, traffic conditions, and waterway conditions.

6 Conclusions and further research

To address the need of the inland waterway transport sector to improve the energy efficiency and increase smart navigation we propose an MPC-based (dynamic) speed planning method. Currently, static speed planning methods are used for inland waterway navigation which are unable to adequately deal with dynamic waterway conditions. The proposed dynamic speed planning continually uses the most up-to-date information on water depth, current speed and expected delays of the journey to re-optimize the speed planning leading to improved energy efficiency, reliable arrival times, and accurate considerations regarding safety.

Compared to a static speed planning method we showed a 8.33% energy reduction, and compared to an adaptive speed selection by a shipper unassisted by optimization strategies we show a 4.31% energy reduction. The energy efficiency percentages achieved with the MPC strategy are a function of the magnitude of the change of the dynamic parameters during the journey. Therefore, the achievable energy reduction through this dynamic speed planning is proportional to the variability and uncertainty experienced during the journey. We also showed that using the proposed method accurate arrival times are achieved compared to static speed planning. Additionally, taking into account the most recent information on water depth and squat as a function of vessel speed, we showed that different speeds are considered safe on the segments of the journey than initially anticipated.

In future work it would be worthwhile to model the uncertainty regarding the expected dynamic conditions. Currently, the expected traffic delay is simply modelled as a proportional delay on travel time which is not accurate enough. Additionally, it would be interesting to see this framework used with prediction models for the water depth, current, and traffic; this could further improve the performance of the dynamic speed planning as indications of future states can be used in planning. Moreover, the effect of locks and their delays should be taken into account also. Considering these improvements the MPC-based speed planning becomes an even more attractive option for energy-efficient and accurate planning.

Acknowledgement

This project is supported by the NWO project 'PATH2ZERO: Transition to Zero-Emission Inland Shipping' (NWA.1439.20.001).

References

Buchem, M., Golak, J.A.P., Grigoriev, A., 2022. Vessel velocity decisions in inland waterway transportation under uncertainty. European Journal of Operational Research 296, 669 – 678. doi:10.1016/j.ejor.2021.04.026. cited by: 6; All Open Access, Hybrid Gold Open Access.

CCNR, 2022. Ccnr roadmap for reducing inland navigation emissions. URL: https://www.ccr-zkr.org/12090000-en.html.

De Ruiter, J.M., Bhoraskar, A., Ligterink, N.E., 2023. Meten op Schepen- Reductiepotentieel van de milieu- en klimaatimpact van binnenvaart , 1–86.

EC, 2020. The european green deal - striving to be the first climate-neutral continent. URL: https://commission.europa.eu/strategy-and-policy/priorities-2019-2024/european-green-deal_en.

EC, 2021. Future-proofing european inland waterway transport - naiades iii action plan. URL: https://transport.ec.europa.eu/transport-modes/inland-waterways/promotion-inland-waterway-transport/naiades-iii-action-plan_en#:~:text=The%20core%20objectives%20are%20to,zero%2Demission%20barges%20by%202050.

EC, 2022. Energy efficiency targets. URL: https://energy.ec.europa.eu/topics/energy-efficiency/energy-efficiency-targets-directive-and-rules/energy-efficiency-targets_en.

Fan, A., Wang, Z., Yang, L., Wang, J., Vladimir, N., 2021. Multi-stage decision-making method for ship speed optimisation considering inland navigational environment. Proceedings of the Institution of Mechanical Engineers, Part M: Journal of Engineering for the Maritime Environment 235, 372–382. URL: https://doi.org/10.1177/1475090220982414, doi:10.1177/1475090220982414, arXiv:https://doi.org/10.1177/1475090220982414.

Gao, J., Chi, M., Hu, Z., 2022. Energy consumption optimization of inland sea ships based on operation data and ensemble learning. Mathematical Problems in Engineering 2022, 1–13. doi:10.1155/2022/9231782.

Han, C., Liu, J., Liu, Z., Li, S., Qin, X., 2021. Research on speed optimization of inland vessels based on a shuffled frog-leaping algorithm, in: 2021 6th International Conference on Transportation Information and Safety (ICTIS), pp. 688–693. doi:10.1109/ICTIS54573.2021.9798521.

Holtrop, J., 1984. A statistical re-analysis of resistance and propulsion data. International Shipbuilding Progress 31.

Holtrop, J., Mennen, G., 1982. An approximate power prediction method. International Shipbuilding Progress 29.

Jiang, M., Segers, L.M., Van der Werff, S.E., Baart, F., Van Koningsveld, M., 2022. Opentnsim-energy .

Kirichek, A., Pruyn, J., Atasoy, B., R. Negenborn, R., Zuidwijk, R., van Duin, J., Tachi, K., van Koningsveld, M., 2024. Paving the way towards zero-emission and robust inland shipping URL: https://proceedings.open.tudelft.nl/moses2023/article/view/675, doi:10.59490/moses.2023.675.

van Koningsveld, M., van der Werff, S., Jiang, M., Lansen, A., de Vriend, H., 2021. Part IV - Ch 5 Performance of ports and waterway systems. TU Delft OPEN Publishing.

Liu, T., 2023. Speed optimization of inland sea vessels based on c.w saving algorithm. Applied Mathematics and Nonlinear Sciences URL: https://sciendo.com/article/10.2478/amns.2023.2.00271, doi:10.2478/amns.2023.2.00271.

NOVIMOVE, 2020. Smart and sustainable waterways. URL: https://novimove.eu/.

Orlovius, V., 1994. Regulations and Prescriptions for the Navigation on the Rhine , 1–16.

Psaraftis, H.N., Kontovas, C.A., 2013. Speed models for energy-efficient maritime transportation: A taxonomy and survey. Transportation Research Part C: Emerging Technologies 26, 331 – 351. doi:10.1016/j.trc.2012.09.012.

Serban, S., Cosmin, K., Panaitescu, V., 2015. The analysis of squat and underkeel clearance for different ship types in a trapezoidal crosssection channel 77, 205–212.

Simić, A., Radojcic, D., 2013. On energy efficiency of inland waterway self-propelled cargo vessels. FME Transactions 41, 138–145.

Sun, L., Zhang, Y., Ma, F., Ji, F., Xiong, Y., 2023. Energy and speed optimization of inland battery-powered ship with considering the dynamic electricity price and complex navigational environment. Energy Reports 9, 293–304. URL: https://www.sciencedirect.com/science/article/pii/S2352484723006297, doi:https://doi.org/10.1016/j.egyr.2023.04.267. 2022 The 3rd International Conference on Power Engineering.

TNO, VIA, PRO, DST, BAW, 2016. PROMINENT - D5.6 Land based tool for evaluation of ship efficiency and navigation performance , 1–29.

WANG, K., LI, J., HUANG, L., Ma, R., QU, X., YUAN, Y., 2019. An energy efficiency optimization method for inland ship fleet considering multiple influencing factors, in: 2019 5th International Conference on Transportation Information and Safety (ICTIS), pp. 1263–1267. doi:10.1109/ICTIS.2019.8883776.

Wang, K., Xu, H., Li, J., Huang, L., Ma, R., Jiang, X., Yuan, Y., Mwero, N.A., Sun, P., Negenborn, R.R., Yan, X., 2021. A novel dynamical collaborative optimization method of ship energy consumption based on a spatial and temporal distribution analysis of voyage data. Applied Ocean Research 112, 102657. URL: https://www.sciencedirect.com/science/article/pii/S0141118721001346, doi:https://doi.org/10.1016/j.apor.2021.102657.

Wang, K., Yin, M., Ayisi, A.D., 2023. Effects of reduced speed on the benefits and pollution of yangtze river ships. Transportation Research Record 2677, 783–796. URL:

https://doi.org/10.1177/03611981221150417, doi:10.1177/03611981221150417, arXiv:https://doi.org/10.1177/03611981221150417.

Yan, X., Wang, K., Yuan, Y., Jiang, X., Negenborn, R.R., 2018. Energy-efficient shipping: An application of big data analysis for optimizing engine speed of inland ships considering multiple environmental factors. Ocean Engineering 169, 457–468. URL: https://www.sciencedirect.com/science/article/pii/S0029801818316421, doi:https://doi.org/10.1016/j.oceaneng.2018.08.050.

Zeng, Q., 2019. A method to improve the prediction of ship resistance in shallow water. Ph.D. thesis. TU Delft.

Zhang, L., Peng, X., Liu, Z., Wei, N., Wang, F., 2022. An application of augmented lagrangian differential evolution algorithm for optimizing the speed of inland ships sailing on the yangtze river. International Journal of Naval Architecture and Ocean Engineering 14, 100488. URL: https://www.sciencedirect.com/science/article/pii/S2092678222000541, doi:https://doi.org/10.1016/j.ijnaoe.2022.100488.

Zhang, Y., Sun, L., Fan, T., Ma, F., Xiong, Y., 2023. Speed and energy optimization method for the inland all-electric ship in battery-swapping mode. Ocean Engineering 284, 115234. URL: https://www.sciencedirect.com/science/article/pii/S0029801823016189, doi:https://doi.org/10.1016/j.oceaneng.2023.115234.